Modulation of FXYD Interaction with Na,K-ATPase by Anionic Phospholipids and Protein Kinase Phosphorylation†

Flemming Cornelius* and Yasser A. Mahmmoud

Department of Biophysics, Institute of Physiology and Biophysics, University of Aarhus, Aarhus 8000, Denmark

Received October 30, 2006; Revised Manuscript Received January 2, 2007

ABSTRACT: FXYD10 is a 74 amino acid small protein which regulates the activity of shark Na,K-ATPase. The lipid dependence of this regulatory interaction of FXYD10 with shark Na,K-ATPase was investigated using reconstitution into DOPC/cholesterol liposomes with or without the replacement of 20 mol % DOPC with anionic phospholipids. Specifically, the effects of the cytoplasmic domain of FXYD10, which contains the phosphorylation sites for protein kinases, on the kinetics of the Na,K-ATPase reaction were investigated by a comparison of the reconstituted native enzyme and the enzyme where 23 C-terminal amino acids of FXYD10 had been cleaved by mild, controlled trypsin treatment. Several kinetic properties of the Na,K-ATPase reaction cycle as well as the FXYD-regulation of Na,K-ATPase activity were found to be affected by acidic phospholipids like PI, PS, and PG. This takes into consideration the Na^+ and K^+ activation, the K^+-deocclusion reaction, and the poise of the E_1/E_2 conformational equilibrium, whereas the ATP activation was unchanged. Anionic phospholipids increased the intermolecular cross-linking between the FXYD10 C-terminus (Cys74) and the Cys254 in the Na,K-ATPase A-domain. However, neither in the presence nor in the absence of anionic phospholipids did protein kinase phosphorylation of native FXYD10, which relieves the inhibition, affect such cross-linking. Together, this seems to indicate that phosphorylation involves only modest structural rearrangements between the cytoplasmic domain of FXYD10 and the Na,K-ATPase A-domain.

FXYD proteins are small, single membrane spanning proteins defined by an invariant extracellular FXYD motif in the N-terminal part (*1*). Seven mammalian species and one species from shark have been characterized so far and have all been demonstrated to regulate the activity of the Na,K-ATPase in various tissues (for reviews, see refs *2*−*4*). There seem to be two groups of FXYD proteins defined according to their capability to be phosphorylated by protein kinases. Indeed, phospholemman (FXYD1 or PLM)[1] in heart and skeletal muscle, the shark rectal gland FXYD10 (PLMS), and possibly the brain specific FXYD7 all contain phosphorylation sites for PKA and PKC (*5*−*8*) located within the cytoplasmic (C-terminal) part of the molecule. Thus, it has been suggested that this group of FXYD proteins can interact dynamically with Na,K-ATPase depending on the protein's phosphorylation state (*2*) resembling the mechanism by which phospholamban (PLB) inhibition of the cardiac isoforms of the sarco(endo)plasmic reticulum Ca^{2+}-ATPase (SERCA2a) is relieved by protein kinase phosphorylation (*9*). It is unclear how PLB phosphorylation affects its interaction with SERCA, but several studies using cross-linking or co-immunoprecipitation imply that phosphorylation of PLB does not interrupt completely physical interactions with SERCA (*10*, *11*). Other experimental evidence has demonstrated that the cytoplasmic domain of free PLB acts as a conformational switch alternating between contacts to the lipid head groups of the membrane surface and to SERCA (*12*), but it is unclear how this relates to the physiological regulation including phosphorylation. It was recently hypothesized from experiments demonstrating the binding of synthetic fragments of the cytoplasmic domain of phospholemman (FXYD1) to lipid membrane surfaces (*13*) that a similar mechanism could be operating in the FXYD regulation of Na,K-ATPase .

The work presented here investigates the effects of phospholipids on the functional regulation of shark Na,K-ATPase by FXYD10. To address the question of the mechanism of protein kinase phosphorylation further, we have reconstituted Na,K-ATPase with full-length or C-terminal truncated FXYD10, in which the multisite phosphorylation domain has been removed by controlled trypsin cleavage into liposomes containing the zwitterionic DOPC and cholesterol in the presence or absence of anionic phospholipids. Several functional properties of Na,K-ATPase were investigated including the apparent affinities for ATP, Na^+, and K^+ as well as the E_1/E_2 conformational poise and the K^+-deocclusion reaction. The structural interactions of FXYD10 with Na,K-ATPase in these different lipid environments were investigated using intermolecular cross-linking with the homobifunctional sulfhydryl cross-linker 1,4-

† This work was supported by grants from The Danish Research Council, the Aarhus University Research Foundation, The Novo Nordisk Foundation, and the A.P. Møller Foundation.

* Corresponding author. Tel.: +4589422926. Fax: +4586129599. E-mail: fc@biophys.au.dk.

[1] Abbreviations: BMDB, 1,4-bismaleimidyl-2,3-dihydrobutane; DOPC, 1,2-dioleoyl-*sn*-glycero-3-phosphocholine; DOPG or PG, 1,2-dioleoyl-*sn*-glycero-3-phospho-*rac*-(1-glycerol); PI, L-α-dioleoylphosphatidylinositol; PS, L-α-dioleoylphosphatidylserine; Chol, cholesterol; PKA, cAMP dependent protein kinase; PKC, Ca^{2+} and phospholipid dependent protein kinase; PLB, phospholamban; PLM, phospholemman; SERCA, sarco(endo)plasmic reticulum Ca-ATPase.

10.1021/bi062239j CCC: $37.00
Published on Web 02/09/2007

bismaleimidyl-2,3-dihydro-butane (BMDB), which links Cys74 in the cytoplasmic domain of FXYD10 to Cys254 in the A-domain of Na,K-ATPase (*14*). Several functional properties dependent on the FXYD interactions, including the maximum turnover number, the apparent cation affinities for Na^+ and K^+, and the K^+-deocclusion step, were found to be influenced by the negative surface charge of liposomes containing anionic phospholipids. Cross-linking efficiency was used to probe significant changes in the spatial location of the cytoplasmic domain of FXYD10 following PKA and PKC phosphorylation.

These observations provide the first direct evidence that the cytoplasmic part of FXYD10 is responsible for the lipid-dependent regulation of several kinetic properties of Na,K-ATPase.

EXPERIMENTAL PROCEDURES

Materials. Highly purified phospholipids, 1,2-dioleoyl-*sn*-glycero-3-phosphocholine (DOPC), L-α-dioleoyl phosphatidylinositol (PI), L-α-dioleoyl phosphatidylserine (PS), or 1,2-dioleoyl-*sn*-glycero-3-phospho-*rac*-(1-glycerol) (DOPG), were obtained from Avanti Polar Lipids. Cholesterol was obtained from Sigma. ATP, purchased as the sodium salt from Roche, was converted to the Tris salt by chromatography on a Dowex 1 column (Sigma). γ-[^{32}P]-ATP was obtained from Amersham, and nigericin was obtained from Molecular Probes. The catalytic subunit of PKA was purchased from Sigma. PKC was obtained from CalBiochem (La Jolla, CA) and contained the Ca^{2+}-dependent (conventional) isoforms (α, β_I, β_{II}, and γ). 1,4-Bismaleimidyl-2,3-dihydrobutane (BMDB) was obtained from Pierce.

Na,K-ATPase Preparation and Hydrolytic Activity. In this study, purified Na,K-ATPase-containing membranes from the rectal gland of *Squalus acanthias* were used. Purification of membrane fragments was performed as previously described (*15*). Protein concentrations, ranging from 3 to 5 mg/mL, were determined using Peterson's modification (*16*) of the Lowry method (*17*), using bovine serum albumin (BSA) as the standard. The specific activity was ~30 U/mg at 37 °C and 10.5 U/mg at 24 °C (1 U = 1 μmol P_i/min). The ATPase activity was measured either by a radioactive assay (at sub-saturating ATP) in a reaction mixture containing 30 mM histidine, pH 7.4, 3 mM $MgCl_2$, 0.06% BSA, 10% glycerol, and 1−1000 μM ATP (containing 0.03 μCi γ-[^{32}P]-ATP) or at saturating ATP (3 mM) by the method of Baginsky et al. (*18*) and with variable concentrations of NaCl, KCl, and ATP as indicated in separate figure legends. The turnover number of the enzyme (molar activity, k_{cat}) was calculated from the protein content, and the determined site number (nanomoles per milligram of protein) was measured as the maximum phosphorylation level attained in 25 μM ATP, 1 mM Mg^{2+}, and 150 mM Na^+ as previously described (*19*).

Gel Electrophoresis and Immunoblotting. The phosphorylated proteins were separated using tricine-based sodium dodecyl sulfate polyacrylamide gel electrophoresis (SDS-PAGE; 3% loading gel, 8% intermediate, and 15% resolving gels). Molecular weight standards were obtained from BioRad (Hercules, CA). For immunoblotting, proteins were transferred to poly(vinylidene difluoride) (PVDF) membranes, then washed for 1 h with phosphate-buffered saline (PBS) buffer containing 5% Tween-20, and incubated overnight at room temperature with primary antibody. The membranes were washed again with PBS and incubated with goat anti-rabbit antibody for 2 h. After washing, the proteins were detected using electrochemical luminescence (ECL) reagents (Amersham Pharmacia). For the detection of the α-subunit from the shark rectal gland, the C-terminal specific antibody NKA1002-1016 was used (kindly provided by Jesper V. Møller, Department of Biophysics, University of Aarhus). For detection of FXYD10, an anti-FXYD10 antiserum was used. The anti-FXYD10 antiserum was prepared as previously described (*20*).

Reconstitution. Functional reconstitution of shark Na,K-ATPase was achieved as previously described (*21*−*23*). Initially membrane bound Na,K-ATPase was solubilized using the non-ionic detergent $C_{12}E_8$. The lipids of choice were solubilized using the same detergent, and the two solutions were mixed at a protein/lipid weight ratio estimated to give a final ratio of 1:20. The detergent was subsequently removed by the addition of hydrophobic bio-beads, and liposomes containing reconstituted Na,K-ATPase spontaneously formed. Careful control during enzyme solubilization ensured that the reconstitution took place without loss of catalytic activity or ion-transport capacity (*20*). Unless otherwise stated, the proteoliposomes were produced in 30 mM NaCl, 2 mM $MgCl_2$, 200 mM sucrose, and 30 mM histidine, pH = 7.0.

Protein determination of reconstituted ATPase was performed according to the Peterson modification (*16*). In this, the reconstituted protein was quantitatively precipitated with sodium deoxycholate and trichloroacetic acid followed by re-suspension in water. SDS was included in the copper tartrate solution to leave the lipid transparent and non-interfering. BSA was run as the standard.

For each proteoliposome preparation, the hydrolytic activity of the inside-out oriented enzyme was measured in the presence of nigericin (1 μM) to equilibrate the liposomes with external K^+ after pre-incubation in MgPi (4 mM) and ouabain (1 mM) to inhibit the enzyme oriented with the extracellular side exposed.

Determination of the phosphorylation site number of the inside-out enzyme was determined as previously described (*19*). Liposomes were pre-incubated with 1 mM ouabain as described above, and phosphorylation was conducted by the addition of 25 μM [^{32}P]ATP in a mixture of 30 mM imidazole, pH 7.4, 2.5 mM $MgCl_2$, 0.5 mM Pi, 72.5 mM NaCl, 115 mM sucrose, and 1 mM ouabain. The reaction time was 20 s at 0 °C. Phosphorylation was terminated by the addition of an acid stop-solution containing 10% TCA, 100 mM phosphoric acid, and 10 mM sodium pyrophosphate. Radioactivity and protein were determined in the precipitate after resuspension in 1 M NaOH at 55 °C. The turnover number of the inside-out oriented enzyme is then calculated by dividing the specific hydrolytic activity with the site number.

Cross-Linking. BMDB is a soluble homobifunctional sulfhydryl cross-linker with a flexible spacer arm with an average span of ~10 Å (*24*). Cross-linking was performed essentially as previously described (*14*). Cross-linking reactions were performed with 9−12 μg protein in 20 mM *N*-(2-hydroxyethyl)piperazine-*N*′-ethanesulfonic acid (Hepes) buffer, pH 6.5 containing 2 mM ethylenediaminetetraacetic acid (EDTA), 20% glycerol, and 0.1−0.4 mM BMDB (from a 20 mM stock solution in $MeSO_4$). The reaction was

conducted at 24 °C for 25 min and terminated by adding a cysteine solution to a final concentration of 2 mM. The samples were incubated for 5 min at 24 °C. They were then treated with SDS sample buffer (*25*) and briefly incubated at 37 °C before loading to SDS gels. Cross-linking products were detected by immunoblotting with anti-FXYD10 antiserum or C-terminal specific Na,K-ATPase antibody.

Phosphorylation with PKA and PKC. PKA phosphorylation was performed in a reaction mixture containing 50 mM Hepes, 10 mM $MgCl_2$, 1 mM ethylene glycol bis(2-aminoethyl ether)-*N*,*N*,*N*′,*N*′-tetraacetic acid (EGTA), 0.1 mM ATP (Tris salt) containing γ-[^{32}P]-ATP (3 μCi/pmol), 10 μg of reconstituted protein, and 2 mU of PKA. PKC phosphorylation was performed in a typical assay mixture containing 50 mM Hepes, 10 mM $MgCl_2$, 0.5 mM $CaCl_2$, 20 μM L-α phosphatidylserine, 10 μM dioleoyl 1,2-*sn*-glycerol, 1 mM ATP, 10 μg of reconstituted protein, and 0.13 μg of purified PKC. The phosphorylation reaction was initiated by the addition of ATP, was allowed to proceed for 30 min at 24 °C, and was terminated by a fivefold dilution of the phosphorylation products with the cross-linking assay medium (see above).

FXYD Truncation by Trypsin Treatment. In order to obtain cleavage of the C-terminus of FXYD10, the membrane-bound enzyme was incubated with trypsin (1:1000 w/w trypsin/protein) for 0−10 min on ice in the presence of 130 mM NaCl or 20 mM KCl and 1 mM EDTA. The reaction was started by the addition of trypsin and was stopped by a 30-fold dilution in 100 mM $KHCO_3$ followed by centrifugation at 170 000*g* for 1 h. This effectively removes any membrane associated trypsin (*26*). The membranes were washed with imidazole buffer (25 mM), centrifuged again, then finally suspended in a 30 mM histidine buffer, pH 7.4 containing 25% glycerol, and stored at −20 °C. All procedures were carefully performed on ice.

Digital Imaging. Analysis of SDS gels and immunoblots were performed using ImageQuant TL software (Amersham Biosciences).

Statistics. Results are expressed as the mean ± standard error of the mean (SEM). A comparison between best-fit values was performed using an F-test, and $p < 0.05$ was considered significant.

RESULTS

Functional reconstitution was performed with the control enzyme and the enzyme treated with trypsin to obtain specific C-terminal cleavage of FXYD10 at Lys51 (*14*). The lipid composition of the liposomes were either DOPC/Chol (0.6:0.4 mol/mol) or DOPC/Chol with 20 mol % anionic phospholipid (PI, PS, or DOPG) replacing DOPC.

Figure 1 shows an immunoblot of the two enzyme preparations (control or FXYD-truncated) reconstituted into DOPC/Chol or DOPC/PI/Chol liposomes using a C-terminal specific antibody to the Na,K-ATPase or anti-FXYD10 antiserum. As seen, the same pattern was observed for the two lipid compositions used, including the expected shift in the FXYD10 position toward a lower molecular mass (from ~15 to ~10 kDa, lanes 1 and 2 in the right panel) following C-terminal cleavage at Lys51 (*20*). As seen from the left panel, the mobility of the α-subunit was not changed; furthermore, following FXYD truncation, the number of phosphorylation sites was also unaffected (typically 2.2 nmol·mg^{-1}) indicating that the Na,K-ATPase remained intact after this mild trypsin treatment.

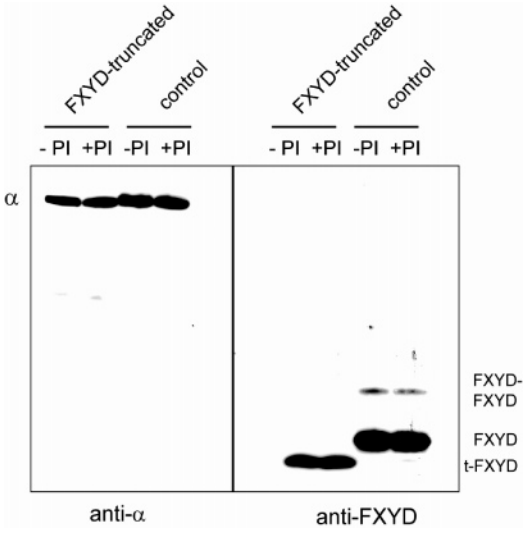

FIGURE 1: Immunoblot of reconstituted Na,K-ATPase containing native or C-terminal truncated FXYD10 (t-FXYD). The left panel shows proteoliposomes immunoblotted with Na,K-ATPase antibody, and the right panel shows proteoliposomes immunoblotted with anti-FXYD10 antiserum. Lanes 1 and 2 are the FXYD-truncated (t-FXYD) enzyme reconstituted into DOPC/Chol (lane 1) or DOPC/PI/Chol liposomes (lane 2). Lanes 3 and 4 are the control enzyme reconstituted into DOPC/Chol (lane 3) or DOPC/PI/Chol liposomes (lane 4). The phosphorylation site numbers for the enzyme reconstituted into DOPC/Chol liposomes were 0.782 ± 0.003 nmol/mg and 0.825 ± 0.006 nmol/mg for the control and the FXYD-truncated enzyme, respectively. For DOPC/PI/Chol liposomes the site numbers were 0.713 ± 0.012 nmol/mg and 0.775 ± 0.008 nmol/mg, respectively (mean ± standard deviation for three experiments). Data are representative of three independent experiments using different proteoliposome preparations.

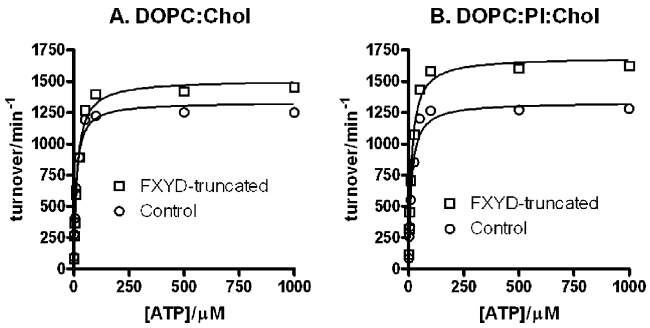

FIGURE 2: ATP activation of the control and FXYD-truncated Na,K-ATPase reconstituted into liposomes without (A) and with (B) PI. The curves represent best fit to the data using a one site binding equation (simple hyperbola). The best-fit values (k_{cat} and K'_{ATP}) in panel A are as follows: control, 1310 ± 19 min^{-1} and 10.2 ± 0.7 μM; and FXYD-truncated, 1512 ± 21 min^{-1} and 14.6 ± 0.9 μM. Those in panel B include control, 1356 ± 24 min^{-1} and 13.0 ± 1.0 μM; and FXYD-truncated, 1694 ± 20 min^{-1} and 13.0 ± 0.7 μM. The calculated apparent ATP affinities were independent of the presence of PI both for controls ($p = 0.054$) and for FXYD-truncated preparations ($p = 0.144$).

In Figure 2, the turnover is measured versus the ATP concentration for the control and FXYD-truncated enzyme reconstituted into two liposome preparations (DOPC/Chol or DOPC/PI/Chol), and the apparent ATP affinity, K'_{ATP}, is calculated by fitting the data with a simple hyperbolic function. The Na^+, K^+, and Mg^{2+} concentrations were 95 mM, 10 mM, and 2 mM, respectively. The best-fit values

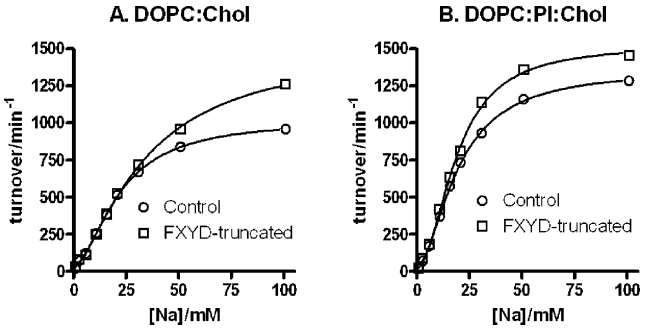

FIGURE 3: Na^+ activation of the control and FXYD-truncated Na,K-ATPase reconstituted into liposomes without (A) or with (B) PI. The curves represent best fit to the data using the Hill equation $v = (k_{cat} - v_0)/(1 + 10^{(\log K_{0.5} - X)n_H}) + v_0$ where $K_{0.5}$ is the Na^+ concentration (X in mM) that gives a turnover (v) halfway between baseline (v_0) and maximum response (k_{cat}) and n_H, the Hill coefficient, is the steepness of the curve. The fitting parameters used in panel A are control enzyme, $k_{cat} = 1025 \pm 19$ min^{-1}, $K_{0.5} = 21.9 \pm 0.2$ mM, and $n_H = 1.74 \pm 0.08$; and for FXYD-truncated enzyme, $k_{cat} = 1514 \pm 46$ min^{-1}, $K_{0.5} = 34.5 \pm 0.5$ mM, and $n_H = 1.46 \pm 0.07$. Those in panel B are control enzyme, $k_{cat} = 1362 \pm 12$ min^{-1}, $K_{0.5} = 19.6 \pm 0.1$ mM, and $n_H = 1.74 \pm 0.04$; and for FXYD-truncated enzyme, $k_{cat} = 1525 \pm 19$ min^{-1}, $K_{0.5} = 19.2 \pm 0.1$ mM, and $n_H = 2.01 \pm 0.08$.

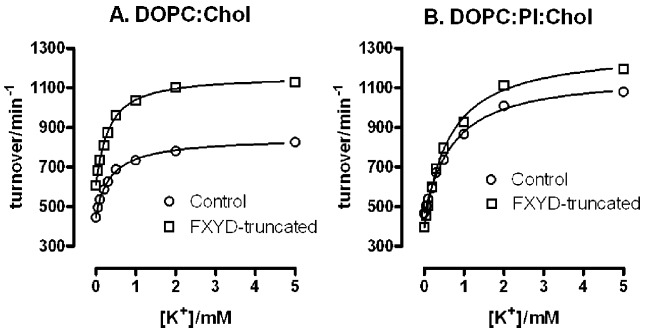

FIGURE 4: K^+ activation of control and FXYD-truncated Na,K-ATPase reconstituted into liposomes without (A) or with (B) PI. The curves represent best fit to the data using the Hill equation. The fitting parameters used in panel A are control enzyme, $k_{cat} = 853 \pm 12$ min^{-1}, $K_{0.5} = 0.37 \pm 0.03$ mM, and $n_H = 0.95 \pm 0.04$; and for FXYD-truncated enzyme, $k_{cat} = 1159 \pm 8$ min^{-1}, $K_{0.5} = 0.31 \pm 0.01$ mM, and $n_H = 1.10 \pm 0.05$. Those in panel B are control enzyme, $k_{cat} = 1158 \pm 19$ min^{-1}, $K_{0.5} = 0.72 \pm 0.14$ mM, and $n_H = 1.12 \pm 0.03$; and for FXYD-truncated enzyme, $k_{cat} = 1294 \pm 24$ min^{-1}, $K_{0.5} = 0.62 \pm 0.09$ mM, and $n_H = 1.05 \pm 0.03$.

(maximum turnover, k_{cat} and K'_{ATP}) were 1310 ± 19 min^{-1} and 10.2 ± 0.7 μM and 1356 ± 24 min^{-1} and 13.0 ± 1.0 μM for the control enzyme reconstituted in DOPC/Chol or DOPC/PI/Chol liposomes, respectively. The same best-fit values for the FXYD-truncated enzyme were 1512 ± 21 min^{-1} and 14.6 ± 0.9 μM and 1694 ± 20 min^{-1} and 13.0 ± 0.7 μM. As previously demonstrated, FXYD truncation activated the maximum hydrolytic activity (*27*), in this case, with 15% and 25% in DOPC/Chol or DOPC/PI/Chol liposomes, respectively. The presence of PI enhanced the activation of maximum turnover of the FXYD-truncated enzyme. The calculated apparent ATP affinities were independent of the presence of PI both for controls ($p = 0.054$) and for FXYD-truncated preparations ($p = 0.144$). The slightly lower K'_{ATP} values found in the present investigation using the reconstituted enzyme compared to previously published values found for shark membrane preparations (cf. refs *7* and *20*) are due to the sidedness of the system with a lower extracellular K^+ concentration (10 mM assuming that nigericin fully equilibrates K^+) and a lower Na^+ concentration inside the liposomes.

The Na^+ and K^+ activations of the control and FXYD-truncated Na,K-ATPase at 100 μM ATP (sub-optimal concentration) reconstituted into DOPC/Chol liposomes or liposomes containing, in addition, PI are shown in Figures 3 and 4 . In the case of Na^+ activation, both k_{cat} and $K'_{0.5}$ increased after FXYD truncation in the absence of PI (Figure 3A). Thus, k_{cat} increased from 1025 to 1514 min^{-1} (48%), and $K'_{0.5}$ increased from 22 to 35 mM. In the presence of PI (Figure 3B), FXYD truncation increased k_{cat} slightly (12% compared with 48%), and $K'_{0.5}$ was unchanged (about 19 mM) and was similar to the control values in the absence of PI. The fitting parameters used for the sigmoid fit (Hill equation) are given in the legend to Figure 3.

In Figure 4, the K^+ activation is shown. In the absence of PI (panel A), turnover increased considerably (36%) after FXYD truncation, as in the case of Na^+ activation. The apparent K^+ affinity was independent of FXYD truncation and was about 0.35 mM. In the presence of PI (panel B), FXYD truncation increased maximum turnover only slightly (12%), and the apparent K^+ affinity was identical (about 0.65 mM), which is twice the value obtained in the absence of PI. Interestingly, FXYD truncation increased the Na^+ activity (i.e., the activity at zero [K^+]) exclusively in the absence of PI.

At physiological conditions, ATP accelerates the K^+-deocclusion reaction $E_2(K_2) \rightarrow E_1ATP$ at the low-affinity site. However, at micromolar concentrations of ATP sufficient to saturate only the high-affinity site, this step becomes rate-limiting in the overall reaction cycle, and K^+ inhibits Na-ATPase activity. Therefore, at micromolar concentrations of ATP, the response of Na-ATPase activity to increasing concentrations of K^+ is a convenient way to assay changes in the $E_2(K_2) \rightarrow E_1$ reaction step (*20*, *28*). We have previously demonstrated that the K^+-deocclusion step is affected by FXYD truncation (*27*). Accordingly, we investigated if this step was sensitive to anionic phospholipids. Figure 5 demonstrates how PI and PG affect the K^+-inhibition profile for the control and FXYD-truncated Na,K-ATPase. For DOPC/Chol liposomes (Figure 5A), the turnover number is decreased by FXYD truncation, and the sensitivity of K^+ inhibition is a little increased following FXYD truncation; however, the difference is not significant (IC_{50} decreases from ~0.58 mM in the control enzyme to ~0.40 mM in the FXYD-truncated enzyme, $p = 0.053$). However, for liposomes with PI (Figure 5B), the pattern is the opposite; the turnover is increased by FXYD truncation, and the sensitivity to K^+ inhibition is decreased instead of increased following FXYD truncation with IC_{50} increasing from ~0.40 mM in DOPC/Chol liposomes to ~0.94 mM when PI is included ($p < 0.0001$). For DOPG liposomes (Figure 5C), the pattern is again different, whereas the control enzyme is inhibited with an IC_{50} of ~0.41 mM; K^+ initially activates enzyme activity of the FXYD-truncated enzyme at low K^+ concentrations, a pattern we have previously observed after FXYD truncation in native membranes (*27*).

The poise of the E_1/E_2 conformational equilibrium of the FXYD-truncated and control Na,K-ATPase reconstituted into DOPC/Chol or DOPC/PI/Chol liposomes was estimated by the sensitivity to vanadate inhibition (*27*, *29*), since vanadate

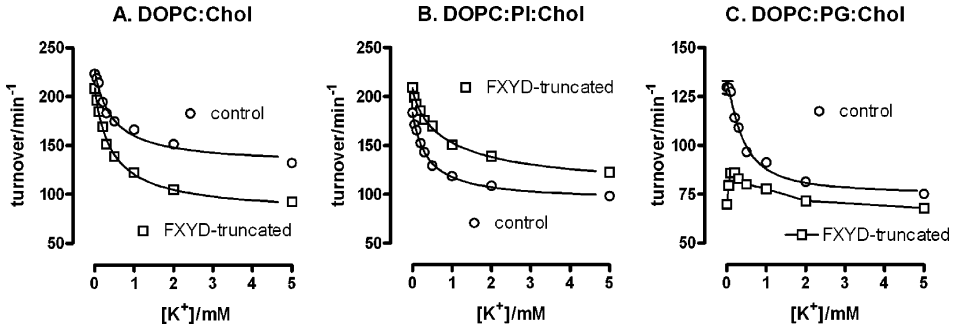

FIGURE 5: K^+ inhibition of Na-ATPase activity at low ATP concentration (1 μM). Results using proteoliposomes containing control and FXYD-truncated Na,K-ATPase without anionic phospholipids (A), with 20 mol % PI (B), or with 20 mol % PG (C) are shown. In panel A, the half-maximal inhibitor concentrations (IC_{50}) are 0.58 ± 0.04 mM and 0.40 ± 0.03 mM for control and FXYD-truncated enzyme, respectively. In panel B, IC_{50} is 0.38 ± 0.03 mM and 0.94 ± 0.05 mM for control and FXYD-truncated enzyme, respectively; and in panel C, IC_{50} is 0.41 ± 0.05 mM for control enzyme.

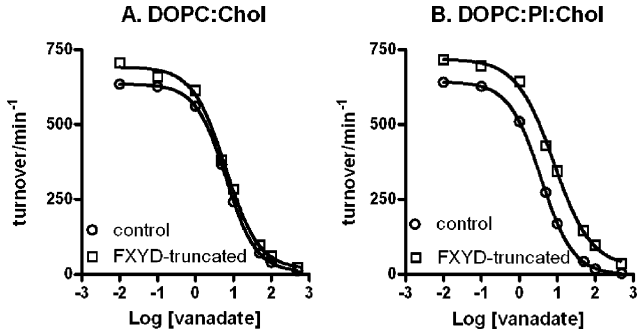

FIGURE 6: Vanadate inhibition of enzyme turnover measured at 10 μM ATP. The curves represent best fit to the data using the Hill equation, $v = (k_{cat} - v_0)/(1 + 10^{((\log K_I - [VO_3])n_H)}) + v_0$, where K_I is the inhibitor concentration ([VO_3] in μM) that gives a turnover (v) halfway between baseline (v_0) and maximum (k_{cat}) values and n_H, the Hill coefficient, is the steepness of the curve. For DOPC/Chol liposomes, the K_I values are control, 6.4 ± 0.2 μM; FXYD-truncated, 6.3 ± 0.2 μM; and DOPC/PI/Chol liposomes, 3.7 ± 0.2 μM and 8.2 ± 0.2 μM. Only the two latter best-fit values are significantly different ($p < 0.0001$).

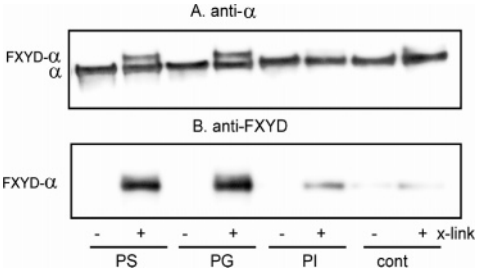

FIGURE 7: Effects of anionic phospholipids on cross-linking of FXYD10 to Na,K-ATPase α-subunit. Immunoblot of Na,K-ATPase reconstituted into DOPC/Chol liposomes without (cont) or with 20 mol % PS, PG, or PI, before and after BMBD cross-linking probed with anti-α antibody (panel A) or anti-FXYD antiserum (panel B). Data are representative of four independent experiments using different proteoliposome preparations. The intensity of cross-linking is clearly increased in the presence of anionic phospholipids, especially by PS and PG. Densitometry of the bands gives a relative intensity per nanomole of the Na,K-ATPase sites (determined from ATP phosphorylation) of control, 1.00; PI, 4.0; PS, 17; and PG, 32.

binds preferentially to the E_2 conformation. As indicated by Figure 6, the poise of the E_1/E_2 conformational equilibrium differed between the control and the FXYD-truncated enzyme only in the presence of PI. Thus, in DOPC/Chol liposomes, the K_I for vanadate was 6.4 ± 0.2 μM and 6.3 ± 0.2 μM for the control and FXYD-truncated enzyme (Figure 6A), whereas in the presence of PI the equivalent values were 3.7 ± 0.2 μM and 8.2 ± 0.2 μM, respectively ($p < 0.0001$, Figure 6B). Thus, in the presence of PI, FXYD truncation shifted the poise in the equilibrium toward the E_1 conformation, as is also the case for PS (K_I for vanadate was 4.3 ± 0.2 μM for the control and 10.9 ± 0.4 μM for the FXYD-truncated enzyme, not shown), for PG (K_I for vanadate was 4.0 ± 0.2 μM for the control and 10.1 ± 0.4 μM for the FXYD-truncated enzyme, not shown), and in native membranes (*20*). In all experiments, the Hill coefficient was found insignificantly different from −1.

As previously demonstrated, protein kinase phosphorylation of both native and reconstituted shark Na,K-ATPase leads to activation at V_{max} conditions (*7*, *30*). Accordingly, we hypothesized that the physiological regulation of Na,K-ATPase by FXYD10 was achieved by structural rearrangements of the FXYD10 interaction with the α-subunit following its phosphorylation in a mechanism resembling the regulation of SERCA by PLB. In order to investigate if the spatial location of the C-terminal domain of FXYD10 was different depending on the presence of anionic phospholipids and depending on the phosphorylation of FXYD10, sulfhydryl cross-linking was performed using BMDB, which has a rather narrow cross-linking range between 9.5 and 13.2 Å (*24*). This cross-linker has previously been shown to cross-link Cys74, the C-terminal cysteine of FXYD10, to Cys254 in the A-domain of the α-subunit (*14*). Thus, cross-linking is expected to decrease if the fluctuations between different FXYD10 conformations (extended or closed, L-shaped) are shifted either by anionic phospholipids or by PKC phosphorylation to stabilize a closed conformation, where the cytoplasmic domain of FXYD10 instead of interacting with the Na,K-ATPase is interfering with the lipid surface.

Figure 7 shows a BMDB cross-linking experiment using Na,K-ATPase reconstituted into DOPC/Chol liposomes (controls) and DOPC/Chol liposomes with either 20 mol % PS or 20 mol % DOPG. After termination of the reactions, samples were subjected to SDS-PAGE followed by immunoblotting with either anti-α or anti-FXYD10 antiserum to detect FXYD10 cross-linked to Na,K-ATPase. As seen from Figure 7, FXYD-α cross-linking was increased in the presence of anionic phospholipids, most obvious when PS and PG are present. Densitometry analysis of the intensity of the cross-linked bands revealed a significant effect of anionic phospholipids on cross-linking efficiency. Thus, in three independent experiments similar to the one depicted

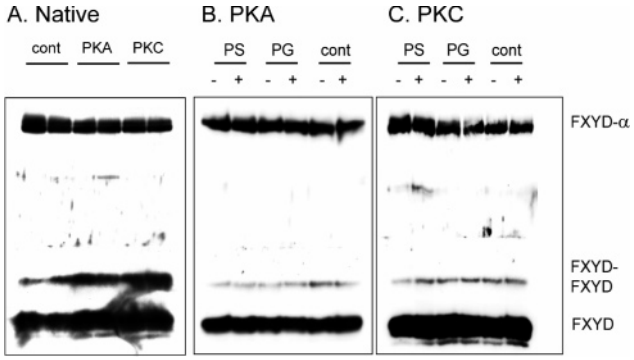

FIGURE 8: Effects of protein kinase phosphorylation on cross-linking of FXYD10 to native and reconstituted Na,K-ATPase α-subunit. Panel A shows the effect of PKA and PKC phosphorylation on FXYD10-Na,K-ATPase cross-linking of native Na,K-ATPase. Panels B and C shows the effects of PKA phosphorylation (B) and PKC phosphorylation (C) on cross-linking of Na,K-ATPase after reconstitution into DOPC/Chol/PS (lanes 1 and 2), DOPC/Chol/PG (lanes 3 and 4), or DOPC/Chol (lanes 5 and 6) liposomes. In the immunoblots, cross-linking was probed using an anti-FXYD antiserum. In panels B and C, lanes 1, 3, and 5 are controls without PKA/PKC phosphorylation. Lanes 2, 4, and 6 are PKA/PKC treated samples. The lower very intense bands represent the 15 kDa FXYD10. Above that, cross-linked FXYD10−FXYD10 is detected, and at the top, FXYD10 cross-linked to the α-subunit is observed at about 100 kDa. Data are representative of three independent experiments using different preparations.

in Figure 7B, normalized FXYD-α band intensities after cross-linking relative to the controls were 4.0 ± 0.3 (PI), 17 ± 0.9 (PS), and 32 ± 0.7 (PG), respectively.

In Figure 8, the effects of PKA and PKC phosphorylation on BMDB cross-linking were compared for enzymes reconstituted in either DOPC/Chol liposomes (controls) or DOPC/Chol liposomes with either 20 mol % PS or 20 mol % DOPG and with a native membrane bound enzyme before reconstitution. As readily observed by comparing the FXYD-α bands before (−) and after (+) protein kinase phosphorylation, neither PKA phosphorylation (panel B) nor PKC phosphorylation (panel C) seriously affected or disrupted the FXYD10-α cross-linking of the reconstituted enzyme at any of the lipid compositions used. The case is the same for the enzyme before reconstitution (panel A), indicating that the position of the C-terminus of FXYD associated with the Na,K-ATPase is not shifted to a position outside the cross-linking range of 9.5−13.2 Å by protein kinase phosphorylation.

DISCUSSION

In the present study, the effects of anionic phospholipids (PI, PS, or PG) on FXYD10 regulation of Na,K-ATPase were investigated. Specifically, the lipid effects on the interaction between the C-terminal domain of FXYD10 and the shark Na,K-ATPase were explored. This was achieved by reconstituting native Na,K-ATPase or Na,K-ATPase where the C-terminal domain of FXYD10 was cleaved by a mild trypsin treatment into liposomes of defined lipid composition (cf. Figure 1). Such a specific cleavage of FXYD10 at Lys51 (see FXYD sequence in Figure 9) can be achieved by trypsin treatment under controlled and mild conditions (low trypsin/protein ratio, short incubation time, and low temperature) without affecting the α-subunit (*27*), as seen from Figure 1. DOPC, together with 40 mol % cholesterol, has previously

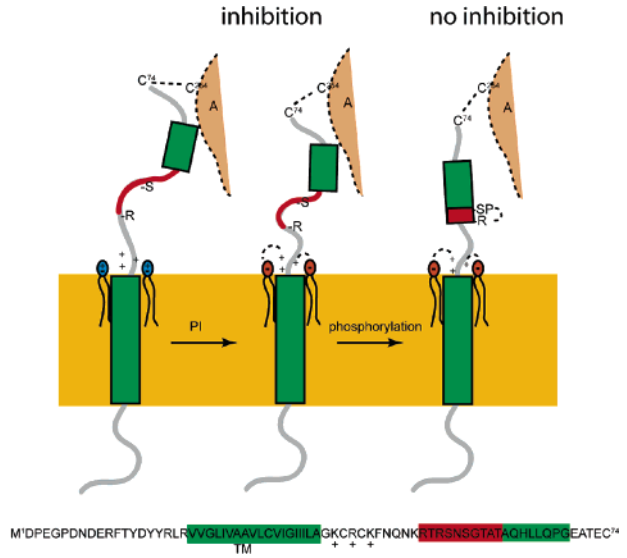

FIGURE 9: Model sketching the interaction between FXYD10 and the Na,K-ATPase. The figure illustrates, on the one hand, the interaction between anionic phospholipids (PI, orange), but not between zwitter-ionic phospholipids (blue), and basic FXYD residues (+, Lys42, Arg44, Lys46) positioned near the lipid surface stabilizing a conformation where the modulation of the Na,K-ATPase is changed, but Cys74 of FXYD (green) is in a more favorable position for cross-linking to Cys254 in the Na,K-ATPase A-domain (light brown). Protein kinase phosphorylation, on the other hand, is assumed to induce formation of salt bridges between phosphorylated serines in the FXYD phosphorylation domain (red) and argenines three amino acids downstream (see sequence below). This stabilizes the helical structure and constrains the overall dimension of the cytoplasmic domain relieving the Na,K-ATPase inhibition. However, the C-terminal Cys74 still remains within the 9.5−12 Å cross-linking distance of BMDB. The sketched mechanism for phosphorylation induced relief of inhibition resembles the model proposed for PLB regulation of SERCA (*42*, *43*), but any model in which salt bridge formation leads to distortions of the FXYD domain that interacts with the Na,K-ATPase, like local helical unwinding (*44*), but retains the spatial organization of Cys74 relative to Cys254 is equally plausible. Below the sketch, the amino acid sequence of the mature FXYD10 is given (GenBank accession number AJ556170).

been demonstrated to support near-maximum activity of purified shark Na,K-ATPase (*31*), and inclusion of acidic phospholipids like PS or PI further increased the Na,K-ATPase activity (*21*). Also, in native shark membrane preparations, spin-labeling experiments have demonstrated a larger specificity of interaction for anionic phospholipids (reviewed by Esman and Marsh (*32*)). Here, we demonstrate that PI (and PS or PG) affected several kinetic steps in the reaction cycle of Na,K-ATPase in a way that depended on the presence of the C-terminal domain of FXYD10. This region contains the multisite protein kinase phosphorylation domain and is implicated in the interaction with the very flexible A-domain of the Na,K-ATPase α-subunit (*14*). As seen from Figure 2, FXYD truncation enhanced the maximum turnover by 15% in the absence of PI but enhanced the maximum turnover by 25% in its presence. The apparent ATP affinity was similar at all conditions, ranging from 10 to 15 μM. Similar results have previously been found with native membrane preparations where FXYD10 truncation also did not affect K'_{ATP} (*27*). Also, the PI effect on cation activation was different for the native and FXYD-truncated enzymes (Figures 3 and 4). The changes in apparent ion affinities are more difficult to evaluate since both $K_{0.5}$ and

k_{cat} change with conditions. However, in the case of Na^+ activation, the ratio $K_{0.5}/k_{cat}$ was independent of FXYD truncation in both the absence and the presence of PI, whereas for K^+ activation this ratio increased in both lipid conditions, indicating that the K^+ affinity has changed (decreased) following FXYD truncation (*33*).

The K^+-deocclusion step $E_2(K_2) \rightarrow E_1$ can be measured as the sensitivity of Na-ATPase for K^+ inhibition at low concentrations of ATP. As shown in Figure 5, the effect of FXYD truncation on this step is strongly dependent on the specific phospholipid composition. In the presence of PI, turnover is increased by FXYD truncation, and IC_{50} for K^+ inhibition is increased by a factor of almost three, from 0.32 to 0.95 mM ($p < 0.0001$); however, in the absence of PI, the turnover is decreased, and IC_{50} is independent of FXYD truncation (IC_{50} is decreased from 0.58 to 0.40 mM, $p = 0.053$). Surprisingly, in the presence of PG, FXYD truncation also resulted in inhibition, but now K^+ initially activated the enzyme. Actually, the IC_{50} values are very similar for the control enzyme at all phospholipid conditions, and the main difference is between FXYD-truncated preparations.

We have previously shown that the K^+-deocclusion step is affected by FXYD10 interactions in native Na,K-ATPase membrane preparations (*27*) and that this step is the main rate-determining step in the overall reaction (*34*, *35*). Together, these results indicate that regulation of this step in the reaction cycle is pivotal in the FXYD10 regulation of Na,K-ATPase activity. Finally, anionic phospholipids are also shown to affect the effect FXYD truncation has on the poise of the E_1/E_2 conformational equilibrium (Figure 6). Thus, in the presence of anionic phospholipids, FXYD truncation shifts the E_1/E_2 poise toward E_1, whereas this is not the case in the absence of PI. It seems, therefore, that the various anionic phospholipids have differentiated effects on certain partial reactions, like the K^+-deocclusion reaction, whereas they all shift the E_1/E_2 conformational poise equally toward E_1. This emphasizes that the steady-state proportion of the E_1 conformation depends on several reaction steps around the catalytic cycle.

Taken together, the results demonstrate that the presence of the anionic phospholipids is important for the detailed kinetics of FXYD regulation of Na,K-ATPase activity. The question is how this is achieved. One hypothesis could be that the C-terminal domain of FXYD10 is interfering with the anionic head group of PI by electrostatic interactions. Such a mechanism would resemble the one believed to work in PLB association with SERCA2a. There, PLB shifts between a free, bend conformation, where the cytoplasmic domain adheres to the lipid surface, and a more extended conformation, where the cytoplasmic domain of PLB is making contact with the cytoplasmic surface of SERCA (*12*, *36*). Results using synthetic fragments representing the cytoplasmic domain of FXYD1 (PLM) demonstrated that these fragments can interact with lipid surfaces containing anionic phospholipids (*13*). The question is, however, whether or not such interactions take place in the native system where the cytoplasmic domain of FXYD is connected with the transmembrane domain and is interacting with the Na,K-ATPase. To answer this question, we investigated whether or not anionic phospholipids decrease the interaction of the C-terminal domain of FXYD with the α-subunit as probed by intermolecular cross-linking. More specifically, the intensity of thiol cross-linking of Cys74 of FXYD10 with Cys254 in the A-domain of the Na,K-ATPase α-subunit was measured in the presence and absence of anionic phospholipids. As seen from Figures 7 and 8, the cross-linking intensity is increased in the presence of anionic phospholipids like PI, PS, or PG, indicating that the interaction between FXYD10 and the Na,K-ATPase α-subunit is stabilized. Thus, either the average spatial distance between the C-terminal domain of FXYD10 and the Na,K-ATPase A-domain could be more favorable in the presence of anionic phospholipids, or the fraction of FXYD associated with Na,K-ATPase is increased. In any case, it definitely does not indicate an increased separation between the FXYD10 C-terminus and the A-domain caused by FXYD alternating between interacting with Na,K-ATPase and interacting with the lipid surface containing anionic phospholipids. It is possible, for example, that electrostatic interactions with the phospholipid head groups of anionic phospholipids and a cluster of basic residues (Lys42, Arg44, Lys46, see Figure 9) in FXYD10 positioned close to the cytoplasmic membrane face stabilize the cytoplasmic FXYD−Na,K-ATPase interaction and favor cross-linking, as depicted in Figure 9. Alternatively, intermolecular interaction at the transmembrane level of FXYD10 could be transmitted from the transmembrane to the cytoplasmic domain of FXYD10 via interactions at the transmembrane level in the bilayer. In both cases, long-range coupling between the transmembrane domain and the cytoplasmic domain would be operating. In the latter case, such long-range coupling could be initiated by changes in the helical packing in the transmembrane domain initiated, for example, by the lateral pressure induced by the lipids (*37*). Such a mechanism would be in accord with the Na,K-ATPase activation observed after the addition of subcritical micellar concentrations of the detergent $C_{12}E_8$ to the Na,K-ATPase membrane preparations (*7*) since the detergent will partition into the lipid bilayer and change the interhelical packing of FXYD10 and Na,K-ATPase at the transmembrane level (*38*). In SERCA, the inhibitory regulation by PLB involves the stabilization of α-helices within the Ca-ATPase transmembrane domain (*39*). Indeed, there must be a long-range coupling throughout the entire FXYD protein from the transmembrane, hydrophobic region to the cytoplasmic C-terminal domain. This does not, however, exclude the fact that any free FXYD10 not associated with Na,K-ATPase could attain a bend conformation with the cytoplasmic domain associated with the lipid surface, as with PLB (*12*).

We have previously demonstrated that phosphorylation of native FXYD10 by protein kinase A (PKA) and C (PKC) relieves the Na,K-ATPase inhibition induced by FXYD10 (*7*). Thus, it was hypothesized that protein kinase phosphorylation could dissociate FXYD10 from the (cytoplasmic) inhibitory interaction sites, probably located on the Na,K-ATPase A-domain as indicated by intermolecular cross-linking results (*14*). This is a similar situation to that found for PLB regulation of SERCA where phosphorylation at Ser16 or Thr17 (*40*, *41*) disrupts the inhibitory PLB−SERCA interaction. It is not known in detail, however, how phosphorylation breaks this interaction, but salt-bridge formation between phosphorylated Ser16 (and Thr17) and nearby positioned arginines (Arg9, Arg13, and Arg14) of PLB, leading to stabilization (*42*, *43*) or unwinding (*44*) of the

cytoplasmic helix, seems to be pivotal in this relief of PLB inhibition. Cross-linking and co-immunoprecipitation experiments have pointed to specific PLB−SERCA interaction sites that are disrupted by PLB phosphorylation (*45*, *46*), but PLB does not dissociate completely from SERCA (*10*, *11*). Interestingly, the present results demonstrate that neither PKA phosphorylation nor PKC phosphorylation of FXYD10 prevented the Cys74−Cys254 cross-linking (Figure 8). Thus, regulatory activation does not lead to a major perturbation of the FXYD10 C-terminus structure following its phosphorylation. It is strongly indicated, by similar results using native shark membrane preparations where cross-linking is also unaffected by protein kinase phosphorylation (Figure 8C), that this is not an artifact due to a change in the conformational flexibility of FXYD10 caused by the reconstitution, per se. Although there must be a dynamic fluctuation among several FXYD conformations, the dissociation of FXYD10 from the inhibitory sites on Na,K-ATPase, possibly located in the A-domain, apparently results in only a minor displacement of the FXYD10 C-terminus, as depicted in Figure 9. This is also in accordance with results from heart muscle cells, where phosphorylation of phospholemman does not inhibit co-immunoprecipitation of PLM and Na,K-ATPase α-subunits (*47*, *48*).

In conclusion, anionic phospholipids themselves influenced not only the detailed kinetics of the Na,K-ATPase reaction mechanism but also the FXYD-regulation of the Na,K-ATPase, most notably the K^+-deocclusion reaction. Furthermore, anionic phospholipids increased Cys74−Cys254 FXYD-α cross-linking in the following ranking, PG ≥ PS > PI. However, neither anionic phospholipids nor FXYD phosphorylation by PKA/PKC, which relieves inhibition of Na,K-ATPase, seems to cause any dramatic spatial rearrangements in the FXYD−Na,K-ATPase interaction, as detected by intermolecular FXYD-α cross-linking. It is not immediately obvious how the interaction between FXYD10 and Na,K-ATPase is disrupted by protein kinase phosphorylation, but it apparently involves only modest structural rearrangements between the cytoplasmic domain of FXYD10 and the Na,K-ATPase A-domain. Thus, any dramatic shift in the dynamic equilibrium toward conformations where the cytoplasmic domain of FXYD10 changes position from interacting with the Na,K-ATPase to interacting with (anionic) phospholipid head groups seems unlikely. Like in PLB regulation of SERCA, phosphorylated FXYD10 remains associated with the Na,K-ATPase.

ACKNOWLEDGMENT

We thank Hanne R. Z. Christensen, Anne Lillevang, and Anne Mette Beck Rasmussen for expert technical assistance.

REFERENCES

1. Sweadner, K. J., and Rael, E. (2000) The FXYD gene family of small ion transport regulators or channels: cDNA sequence, protein signature sequence, and expression, *Genomics 68*, 41−56.
2. Cornelius, F., and Mahmmoud, Y. A. (2003) Functional modulation of the sodium pump: the regulatory proteins "Fixit", *News Physiol. Sci. 18*, 119−124.
3. Garty, H., and Karlish, S. J. D. (2006) Role of FXYD proteins in ion transport, *Annu. Rev. Physiol. 68*, 431−459.
4. Geering, K. (2006) FXYD proteins: new regulators of Na-K-ATPase, *Am. J. Physiol. 290*, F241−F250.
5. Palmer, C. J., Scott, B. T., and Jones, L. R. (1991) Purification and complete sequence determination of the major plasma membrane substrate for cAMP-dependent protein kinase and protein kinase C in myocardium, *J. Biol. Chem. 266*, 11126−11130.
6. Mounsey, J. P., John, J. E., III, Helmke, S. M., Bush, E. W., Gilbert, J., Roses, A. D., Perryman, M. B., Jones, R, L., and Moorman, J. R. (2000) Phospholemman is a substrate for myotonic dystrophy protein kinase, *J. Biol. Chem. 275*, 23362−23367.
7. Mahmmoud, Y. A., Vorum, H., and Cornelius, F. (2000) Identification of a phospholemman-like protein from shark rectal glands. Evidence for indirect regulation of Na,K-ATPase by protein kinase C via a novel member of the FXYDY family, *J. Biol. Chem. 275*, 35969−35077.
8. Mahmmoud, Y. A., Vorum, H., and Cornelius, F., manuscript in preparation.
9. MacLennan, D. H., and Kranias, E. G. (2003) Phospholamban: a crucial regulator of cardiac contractility, *Nat. Rev. Mol. Cell Biol. 4*, 566−577.
10. Asahi, M., McKenna, E., Kurzydlowski, K., Tada, M., and MacLennan, D. H. (2000) Physical interactions between phospholamban and sarco(endo)plasmic reticulum Ca^{1+}-ATPases are dissociated by elevated Ca^{2+}, but not by phospholamban phosphorylation, vanadate, or thapsigargin, and are enhanced by ATP, *J. Biol. Chem. 275*, 15034−15038.
11. Negash, S., Tao, Q., Sun, H., Li, J., Bigelow, D. J., and Squier, T. C. (2000) Phospholamban remains associated with the Ca^{2+}- and Mg^{2+}-dependent ATPase following phosphorylation by cAMP-dependent protein kinase, *Biochem. J. 351*, 195−205.
12. Zamoon, J., Nitu, F., Karim, C., Thomas, D. D., and Veglia, G. (2005) Mapping the interaction surface of a membrane protein: unveiling the conformational switch of phospholamban in calcium pump regulation, *Proc. Natl. Acad. Sci. U.S.A. 102*, 4747−4752.
13. Clayton, J. C., Hughes, E., and Middleton, D. A. (2005) The cytoplasmic domains of phospholamban and phospholemman associate with phospholipid membrane surfaces, *Biochemistry 44*, 17016−17026.
14. Mahmmoud, Y. A., Vorum, H., and Cornelius, F. (2005) Interaction of FXYD10 (PLMS) with Na,K-ATPase from shark rectal glands. Close proximity of Cys^{74} of FXYD10 to Cys^{254} in the A domain of the α-subunit revealed by intermolecular cross-linking, *J. Biol. Chem. 280*, 27776−27782.
15. Skou, J. C., and Esmann, M. (1979) Preparation of membrane-bound and solubilized (Na^++K^+)-ATPase from rectal glands of *Squalus acanthias*. The effect of preparative procedures on purity, specific and molar activity, *Biochim. Biophys. Acta 567*, 436−444.
16. Peterson, G. L. (1977) A simplification of the protein assay method of Lowry et al. which is more generally applicaple, *Anal. Biochem. 83*, 346−356.
17. Lowry, O. H., Rosebrough, N. J., Farr, A. L., and Randall, R. J. (1951) Protein measurement with the folin phenol reagent, *J. Biol. Chem. 193*, 265−275.
18. Baginsky, E. S., Foa, P. P., and Zak, B. (1967) Microdetermination of inorganic phosphate, phospholipids, and total phosphate in biological materials, *Clin. Chim. Acta 13*, 326−332.
19. Cornelius, F. (1995) Phosphorylation/dephosphorylation of reconstituted shark Na^+,K^+-ATPase: one phosphorylation site per $\alpha\beta$ protomer, *Biochim. Biophys. Acta 1235*, 197−204.
20. Cornelius, F., Mahmmoud, Y. A., Meischke, L., and Cramb, G. (2005) Functional significance of the shark Na,K-ATPase N-terminal domain. Is the structurally variable N-terminus involved in tissue-specific regulation by FXYD proteins?, *Biochemistry 44*, 13051−13062.
21. Cornelius, F., and Skou, J. C. (1984) Reconstitution of (Na^++K^+)-ATPase into phospholipid vesicles with full recovery of its specific activity, *Biochim. Biophys. Acta 772*, 357−373.
22. Cornelius, F. (1988) Incorporation of $C_{12}E_8$-solubilized Na^+,K^+-ATPase into liposomes: determination of sidedness and orientation, *Methods Enzymol. 156*, 156−167.
23. Cornelius, F. (1991) Functional reconstitution of the sodium pump. Kinetics of exchange reactions performed by reconstituted Na/K-ATPase, *Biochim. Biophys. Acta 1071*, 19−66.
24. Green, N. S., Reisler, E., and Houk, K. N. (2001) Quantitative evaluation of the lengths of homobifunctional protein cross-linking reagents used as molecular rulers, *Protein Sci. 10*, 1293−1304.
25. Laemmli, U. K. (1970) Cleavage of structural proteins during the assembly of the head of bacteriophage T4, *Nature 227*, 680−685.

26. Mahmmoud, Y. A. (2005) Stabilization of trypsin by association to plasma membranes: implications for tryptic cleavage of membrane-bound Na,K-ATPase, *Biochim. Biophys. Acta 1720*, 110−116.
27. Mahmmoud, Y. A., Cramb, G., Maunsbach, A. B., Cutler, C. P., Meischke, L. M., and Cornelius, F. (2003) Regulation of Na,K-ATPase by PLMS, the phospholemman-like protein from shark, *J. Biol. Chem. 278*, 37427−37438.
28. Daly, S. E., Lane, L. K., and Blostein, R. (1996) Structure/function analysis of the amino-terminal region of the α1 and α2 subunits of Na,K-ATPase, *J. Biol. Chem. 271*, 23683−23689.
29. Boxenbaum, N., Daly, S. E., Javaid, Z. Z., Lane, L. K., and Blostein, R. (1998) Changes in steady-state conformational equilibrium resulting from cytoplasmic mutations of the Na,K-ATPase α-subunit, *J. Biol. Chem. 273*, 23086−23092.
30. Cornelius, F., and Logvinenko, N. (1996) Functional regulation of reconstituted Na,K-ATPase by protein kinase A phosphorylation, *FEBS Lett. 380*, 277−280.
31. Cornelius, F. (2001) Modulation of Na,K-ATPase and Na-ATPase activity by phospholipids and cholesterol. I. Steady-state kinetics, *Biochemistry 40*, 8842−8851.
32. Esmann, M., and Marsh, D. (2006) Lipid-protein interactions with the Na,K-ATPase, *Chem. Phys. Lipids 114*, 94−104.
33. Plesner, I. W. (1986) The apparent K_m is a misleading kinetic indicator, *Biochem. J. 239*, 175−178.
34. Lüpfert, C., Grell, E., Pintschvius, V., Apell, H.-J., Cornelius, F., and Clarke, R. J. (2001) Rate limitation of the Na^+, K^+-ATPase pump cycle, *Biophys. J. 81*, 2069−2081.
35. Humphrey, P. A., Lüpfert, C., Apell, H.-J., Cornelius, F., and Clarke, R. J. (2002) Mechanism of the rate-determining step of the Na^+,K^+-ATPase pump cycle, *Biochemistry 41*, 9496−9507.
36. Toyoshima, C., Asahi, Y., Khanna, R., Tsuda, T., and MacLennan, D. H. (2003) Modeling of the inhibitory interaction of phospholamban with the Ca^{2+} ATPase, *Proc. Natl. Acad. Sci. U.S.A. 100*, 467−472.
37. Cantor, R. S. (1997) Lateral pressures in cell membranes: a mechanism for modulation of protein function, *J. Phys. Chem. B 101*, 1723−1725.
38. Therien, A. G., and Deber, C. M. (2002) Interhelical packing in detergent micelles. Folding of a cystic fibrosis transmembrane conductance regulator construct, *J. Biol. Chem. 277*, 6067−6072.
39. Tatulian, S. A., Chen, B., Li, J., Negash, S., Middaugh, C. R., Bigelow, D. J., and Squiere, T. C. (2002) The inhibitory action of phospholamban involves stabilization of α-helices within the Ca-ATPase, *Biochemistry 41*, 741−751.
40. Simmerman, H. K., Collins, J. H., Theibert, J. L., Wegener, A. D., and Jones, L. R. (1986) Sequence analysis of phospholamban. Identification of phosphorylation sites and two major structural domains, *J. Biol. Chem. 261*, 13333−13341.
41. Fujii, J., Ueno, A., Kitano, K., Tanaka, S., Kadoma, M., and Tada, M. (1987) Complete complementary DNA-derived amino acid sequence of canine cardiac phospholamban. *J. Clin. Invest. 79*, 301−304.
42. Li, J., Bigelow, D. J., and Squier, T. C. (2003) Phosphorylation by cAMP-dependent protein kinase modulates structural coupling between the transmembrane and cytosolic domains of phospholamban, *Biochemistry 42*, 10674−10682.
43. Li, J., Bigelow, D. J., and Squier, T. C. (2004) Conformational changes within the cytosolic portion of phospholamban upon release of Ca-ATPase inhibition, *Biochemistry 43*, 3870−3879.
44. Sugita, Y., Miyashita, N., Yoda, T., Ikeguchi, M., and Toyoshima, C. (2006) Structural changes in the cytoplasmic domain of phospholamban by phosphorylation at Ser16: a molecular dynamic study, *Biochemistry 45*, 11752−11761.
45. James, P., Inui, M., Tada, M., Chiesi, M., and Carafoli, E. (1989) Nature and site of phospholamban regulation of the Ca^{2+} pump of sarcoplasmic reticulum, *Nature 342*, 90−92.
46. Jones, L. R., Cornea, R. L., and Chen, Z. (2002) Close proximity between residue 30 of phospholamban and cysteine 318 of the cardiac Ca^{2+} pump revealed by intermolecular thiol cross-linking, *J. Biol. Chem. 277*, 28319−28329.
47. Fuller, W., Eaton, P., Bell, J. R., and Shattock, M. J. (2004) Ischemia-induced phosphorylation of phospholemman directly activates rat cardiac Na/K-ATPase, *FASEB J. 18*, 197−199.
48. Bossuyt, J., Ai, X., Moorman, R. J., Pogwizd, S. M., and Bers, D. M. (2005) Expression and phosphorylation of the Na-pump regulatory subunit phospholemman in heart failure, *Circ. Res. 97*, 558−565.

BI062239J